Article - Discoveries

The CARD-CC/Bcl10/paracaspase signaling complex is functionally conserved since the last common ancestor of planulozoa.

Jens Staal[1,2], Yasmine Driege[1,2], Paco Hulpiau[1,2], Laurens Lievens[1,2], Ismail Sahin Gul[1,2], Srividhya Sundararaman Iyer[1,2], Frans Van Roy[1,2], Rudi Beyaert[1,2]

[1] Inflammation Research Center, VIB, Ghent, Belgium

[2] Department of Biomedical Molecular Biology, Ghent University, Ghent, Belgium

Keywords: NF-kappaB, inflammation, CYLD, comparative biology

Address for correspondence:

Inflammation Research Center, VIB & Ghent University,

Unit of Molecular Signal Transduction in Inflammation

Technologiepark 927, B-9052 Ghent, Belgium.

Tel: +32.9.3313770; Fax: +32.9.2217673

Acknowledgments
Zebrafish cDNA was kindly provided by Prof. Kris Vleminckx (Ghent University). A pacific oyster (*Crassostrea gigas*) cDNA library was kindly provided by Prof. Pascal Favrel (UMR BOREA Biologie des ORganismes et Ecosystèmes Aquatiques, Institut de Biologie Fondamentale et Appliquée, Université de Caen Basse-Normandie).

Abstract

Type 1 paracaspases originated in the Ediacaran geological period before the last common ancestor of bilaterans and cnidarians (planulozoa). Cnidarians have several paralog type 1 paracaspases, type 2 paracaspases, and a homolog of Bcl10. Notably in bilaterans, lineages like nematodes and insects lack Bcl10 whereas other lineages such as vertebrates, hemichordates, annelids and mollusks do contain Bcl10. A survey of invertebrate CARD-coiled-coil (CC) domain homologs of CARMA/CARD9 revealed such homologs only in species with Bcl10, indicating an ancient co-evolution of the entire CARD-CC/Bcl10/MALT1-like paracaspase (CBM) complex. Furthermore, vertebrate-like Syk/Zap70 tyrosine kinase homologs with the ITAM-binding SH2 domain were found in invertebrate organisms with CARD-CC/Bcl10, indicating that this pathway might be the original user of the CBM complex. We also established that the downstream signaling proteins TRAF2 and TRAF6 are functionally conserved in cnidaria. There seems to be a correlation where invertebrates with CARD-CC and Bcl10 have type 1 paracaspases which are more similar to the paracaspases found in vertebrates. A proposed evolutionary scenario includes two ancestral type 1 paracaspase paralogs in the protostomian last common ancestor, where one paralog usually is dependent on CARD-CC/Bcl10 for its function. Functional analyses of invertebrate type 1 paracaspases and Bcl10 homologs support this scenario and indicate an ancient origin of the CARD-CC/Bcl10/paracaspase signaling complex.

Introduction

The paracaspase MALT1 (PCASP1) was originally identified in humans as an oncogenic fusion with IAP2 in low-grade antibiotic-resistant MALT lymphomas (Dierlamm et al. 1999). Later, it was discovered that MALT1 is a critical component in T and B cell antigen receptor signaling as part of the CARMA1-Bcl10-MALT1 (CBM) complex (Ruefli-Brasse et al. 2003; Ruland et al. 2003; Che et al. 2004). More studies made it clear that MALT1 plays a role in several different CARD*-Bcl10-MALT1 complexes in many different types of signaling pathways, where currently known CARD* components are CARD9 (Gross et al. 2006), CARD11 (CARMA1) (Che et al. 2004), CARD14 (CARMA2) (Afonina et al. 2016; Howes et al. 2016; Schmitt et al. 2016) and CARD10 (CARMA3) (McAllister-Lucas et al. 2007). These four CARD* proteins form a distinct family with low sequence similarity to other CARD proteins. This family is characterized by a CARD and a coiled-coil (CC) domain and will henceforth be referred to as CARD-CC proteins. The use of the different CARD-CC proteins in the CBM complexes is most likely mostly dependent on cell-type specific expression (Scudiero et al. 2013). MALT1 was originally identified as a “paracaspase” due to sequence similarity with the true caspases and “metacaspases” (Uren et al. 2000). The name caspase signifies both the structure (cysteine protease) and function (aspartic acid substrate specificity) of the protein family. The semantic association of metacaspases and paracaspases to caspases is therefore unfortunate, since the similar names inspired false assumptions of common roles and properties of the different protein families (Salvesen et al. 2015). It was not until much later that the proteolytic activity of MALT1 was established (Coornaert et al. 2008; Rebeaud et al. 2008). In contrast to true caspases (but similar to metacaspases and orthocaspases) the paracaspase MALT1 cleaves substrates specifically after an arginine residue (Yu et al. 2011; Hachmann et al. 2012; Wiesmann et al. 2012). Lately, some protein substrates have been identified which are cleaved after a lysine by the API2-MALT1 oncogenic fusion (Nie et al. 2015). MALT1 cleaves itself (Baens et al. 2014) and its interacting adaptor protein Bcl10 (Rebeaud et al. 2008), the anti-inflammatory deubiquitinases A20 (Coornaert et al. 2008) and CYLD (Staal et al. 2011), the NF-κB member RelB (Hailfinger et al. 2011), the ubiquitin ligase HOIL-1 (Elton et al. 2015; Klein et al. 2015; Douanne et al. 2016) and the specific RNA degradation associated proteins Regnase (Uehata et al. 2013) and Roquin (Jeltsch et al. 2014). The anti-inflammatory role of many of the known protease substrates coupled with the critical role for MALT1 in inflammatory signaling has sparked an interest in targeting MALT1 protease activity as a therapeutic strategy treatment of autoimmune diseases. The proteolytic activity of MALT1 was also found to be critical specifically for ABC-DLBCL B-cell lymphomas (Fontan et al. 2012), which has sparked an interest in MALT1 protease activity also as a cancer therapy target. Although MALT1 has been clearly associated to NF-κB activity, its protease activity plays a more subtle role being specifically required for c-Rel activation (Ferch et al. 2007; Gringhuis et al. 2011; Hailfinger et al. 2011; Baens et al. 2014). There is some evidence that MALT1 also regulate or cross-talk with other pathways, such as JNK/AP-1 (Staal et al. 2011), mTORC1 (Hamilton et al. 2014) and possibly WNT (Bognar et al. 2016). MALT1 belongs to the type 1 paracaspase family, which consist of an N-terminal Death domain, immunoglobulin domains and a paracaspase domain (Hulpiau et al. 2015). The type 1 family of paracaspases originated sometime during the Ediacaran geological period, preceding the last common ancestor of bilaterans and cnidarians (Peterson et al. 2004; Knoll et al. 2006; Hulpiau et al. 2015). The cnidarians (e.g. jellyfish, anemone, hydra, coral, ...) and bilaterans (e.g. vertebrates, insects, nematodes, mollusks, ringed worms, …) form the planulozoan clade (Dunn et al. 2014). In our previous survey of paracaspases and MALT1-associated proteins, type 1 paracaspases and Bcl10 could not be found outside planulozoa (Hulpiau et al. 2015). Cnidarians typically contain several paralogs of both type 1 and the ancient type 2 paracaspases whereas bilaterans typically contain a single copy of a type 1 paracaspase. A notable exception is the jawed vertebrates, where the type 1 paracaspase got triplicated. Subsequently, two paralogs were lost in the mammalian lineage leaving PCASP1 (MALT1) as the single paracaspase in mammals (Hulpiau et al. 2015). Importantly, some organisms such as the nematode *Caenorhabditis elegans* contain a conserved type 1 paracaspase but lack NF-κB (Sullivan et al. 2009), which indicate that other roles or mechanisms might be responsible for the conservation of the general domain organization of the type 1 paracaspases (Hulpiau et al. 2015). The WormBase *C. elegans* phenotype database indicates an important role for the type 1 paracaspase (*tm289* vs *tm321* mutant) in nematodes (C. elegans Deletion Mutant Consortium 2012). On the other hand, despite the apparent importance and remarkable conservation of type 1 paracaspases, there are examples of bilaterans that have lost its paracaspase – most notable the group of flies that include the fruit fly *Drosophila melanogaster* (Hulpiau et al. 2015). This indicates that alternative mechanisms can take over the unknown role which is usually filled by the type 1 paracaspases in most other planulozoan organisms. Apart from functional studies of MALT1 in human and mouse models, investigating the evolutionary history of the type 1 paracaspases and its interacting proteins in alternative model systems could provide important clues to yet-unknown roles and functions of MALT1 (Hulpiau et al. 2015). Finding those alternative functions of MALT1 could also be important for future MALT1 inhibitor-based therapies (Demeyer et al. 2016).

Results & Discussion

Correlation vertebrate-like type 1 paracaspases and presence of Bcl10.

While searching for invertebrate homologs of type 1 paracaspases and Bcl10, it became apparent that type 1 paracaspases from species containing Bcl10 generally had higher BLASTP rankings compared to species

from phyla lacking Bcl10. Bcl10 sequences in vertebrates appear to evolve in a manner similar to how the species have diverged throughout evolution, while the invertebrate Bcl10 sequences are poorly resolved (Figure 1A). To get a better understanding of early Bcl10 evolution, more sequences from invertebrate genomes are needed (GIGA community of scientists 2014; Long et al. 2016). Different alignment strategies (Clustal Omega (Sievers and Higgins 2014) , MUSCLE (Edgar 2004), T-Coffee (Notredame et al. 2000)) and phylogenetic analyses (PhyML (Guindon et al. 2009), MrBayes (Ronquist and Huelsenbeck 2003)) of several type 1 paracaspases verify that type 1 paracaspases from species that contain Bcl10 (mollusks, annelids, hemichordates) often cluster closer to the vertebrate paracaspases, either directly or indirectly by clustering with the invertebrate PCASP3 orthologs from tunicate and lancelet (Hulpiau et al. 2015) (Figure 1B), indicating a conserved common Bcl10-dependent ancestor. We can currently not resolve whether there were two paracaspase paralogs, one Bcl10-dependent and the other Bcl10-independent already from the planulozoan last common ancestor or if Bcl10-independent paralogs have evolved several times. In the second model, a Bcl10-independent paralog would have evolved early on in the protostomian evolution. Since the cnidarian paracaspases tend to cluster together in most models, we expect that the last common bilateran ancestor had a single Bcl10-dependent type 1 paracaspase. In contrast to the signs of co-evolution in the type 1 paracaspases, the Bcl10-interacting inhibitory protein CARD19 (BINCA) (Woo et al. 2004) could not be found among invertebrates, while another Bcl10-interacting inhibitory protein, CRADD (Lin et al. 2012), was found in a wide range of organisms and did not correlate with the presence of Bcl10.

Functional conservation of invertebrate type 1 paracaspases

Based on BLASTP and subsequent phylogenetic analyses, the mollusk paracaspases were identified as the non-deuterostome homologs most closely resembling vertebrate type 1 paracaspases (Hulpiau et al. 2015). Based on top-ranking BLASTP hits, the pacific sea oyster (*Crassostrea gigas*) (Zhang et al. 2012) was selected as a model and cDNA source for the mollusks. Conversely, the most distantly related species where type 1 paracaspases and Bcl10 could be found are cnidaria (Hulpiau et al. 2015). The cnidarian model organism starlet sea anemone (*Nematostella vectensis*) (Darling et al. 2005) was used as a cDNA source for as divergent homologous proteins as possible. In order to investigate the functional conservation of invertebrate type 1 paracaspases, we evaluated artificially activated type 1 paracaspases fused to the ETV6 HLH domain (Baens et al. 2014). As positive control, the currently most distantly related vertebrate paracaspase with conserved activity (zebrafish PCASP3) (Hulpiau et al. 2015) was used. In an NF-κB luciferase assay, only the activated zebrafish PCASP3 could induce the reporter to relevant levels, indicating that the pacific oyster (CgPCASP) and the two starlet sea anemone type 1 paracaspase paralogs (NvPCASP-t1A, NvPCASP-t1B) could not recruit critical downstream signaling components (Figure 2A). Although a statistically significant NF-κB induction could be seen from CgPCASP, the levels were more than 150-fold less than what is observed from vertebrate paracaspases and probably not relevant (Figure 2A). CYLD is chosen as model substrate for evaluation of protease activity and specificity since it is a large protein with many potential aspecific cleavage sites, and it represents one of the oldest paracaspase substrates (Hulpiau et al. 2015). Exceptionally, the anemone (*Nematostella* and *Aiptasia*) CYLD homolog is short and roughly correspond to the C-terminal cleavage fragment of human CYLD. Other cnidaria (e.g. the coral *Acropora digitifera* and the hydrozoan *Hydra vulgaris*) show a long form of CYLD which aligns to the full-length sequence of human CYLD. Evaluation of protease activity on the human CYLD substrate revealed that the pacific oyster paracaspase specifically cleaves human CYLD at R324, just like vertebrate paracaspases (Figure 2B). This differs from our previous studies of invertebrate paracaspases such as the type 1 paracaspase from *C. elegans* and the more distantly related type 2 paracaspases, which failed to show any activity (Hulpiau et al. 2015). On the other hand, the “A” and “B” type 1 paracaspase paralogs from starlet sea anemone could not cleave CYLD at all, indicating that paracaspase substrate specificity is not conserved in the cnidarians despite being an organism with a Bcl10 homolog. It is however important to stress that a lack of MALT1-like activity of a distant homolog in a human host cell does not exclude MALT1-like activity in its native cellular environment. Many critical parameters might differ between the cellular environments such as interacting host proteins, post-translational modifications (phosphorylation, ubiquitination, …) and biophysical conditions (temperature, pH, redox state, ion concentrations, …). Previous studies with heterologous expression of cnidarian caspase-8 homologs has however been able to establish functional conservation in a human cellular background (Sakamaki et al. 2014). Nevertheless, we can establish that the MALT1-like protease substrate specificity predates the divergence of deuterostomian and protostomian bilaterans and that the MALT1-like substrate specificity is older than the MALT1-like scaffold function for induction of NF-κB.

Functional conservation of Bcl10-induced MALT1 activity

To further investigate the functional conservation of the Bcl10/paracaspase co-evolution, we transfected human, zebrafish, pacific oyster and starlet sea anemone Bcl10 in MALT1 KO HEK293T cells with or without reconstitution with human MALT1. Strikingly, the starlet sea anemone Bcl10 could induce human MALT1-mediated NF-κB induction. This result is highly unexpected, since a critical MALT1 Ig domain interaction sequence that has been identified downstream of the CARD domain in human Bcl10 (Langel et al. 2008) only can be found in vertebrates. In contrast to human and zebrafish Bcl10, NvBcl10 does not appear to be cleaved by human MALT1 (Figure 2C). The observation that cnidarian Bcl10 can activate human MALT1

indicates a highly conserved interaction surface between the two proteins. A conserved Bcl10-paracaspase interaction was confirmed with yeast-2-hybrid analysis, where the *Nematostella* type 1 "B" paralog readily interacted with both human and *Nematostella* Bcl10. The "A" paralog did not show any interaction and human MALT1 showed much stronger interaction with human Bcl10 compared to *Nematostella* Bcl10 (Figure 2D). This type of conservation could be used to further model the interaction surfaces using evolutionary data (Hopf et al. 2014). The pacific oyster Bcl10 failed to induce any NF-κB reporter activity, which might be due to its small size. The currently annotated pacific oyster Bcl10 homolog only consist of the CARD domain, which has been shown to be insufficient for NF-κB induction in human Bcl10 (Langel et al. 2008). It will be interesting to see if future annotations of the mollusk genomes will establish a longer Bcl10 transcript encoding for a functional Bcl10 homolog (Riviere et al. 2015). From these experiments we can however conclude that the Bcl10/paracaspase interaction is ancient and highly conserved.

Cnidarian-level functional conservation of downstream signaling proteins

Since neither mollusk nor anemone type 1 paracaspases were able to induce NF-κB in a human cellular background, we wanted to investigate whether downstream signaling components are functionally conserved. The TRAF family of E3 ligases are conserved and diverged before the cnidarian/bilateran last common ancestor (Meyer and Weis 2012). In humans, TRAF6 is the critical member of this family for signaling downstream of MALT1. In other signaling pathways or in the API2-MALT1 oncogenic fusion, TRAF2 plays an as important role in NF-κB induction (Noels et al. 2007). The Ig2 TRAF6 binding motif (TDEAVECTE) and the C-terminal (PVETTD) TRAF6-binding site in MALT1 (Noels et al. 2007) are for example PCASP1-specific, but we know that vertebrate PCASP2 and PCASP3 paralogs still are as efficient in NF-κB induction (Hulpiau et al. 2015). One TRAF6 binding (TPEETG) site in human MALT1 appear to be conserved in all vertebrate paralogs, and the corresponding critical glutamic acid might be present in mollusk and cnidarian paracaspases (dependent on alignment algorithm) while it appears to be missing in nematode and arthropod homologs. In order to investigate whether the type 1 paracaspase – TRAF interaction has undergone lineage-specific divergence, we cloned the *Nematostella* homologs of TRAF2 and TRAF6 and co-expressed them with the two *Nematostella* type 1 paracaspase paralogs fused to the activating ETV6 HLH domain in an NF-κB luciferase assay (Figure 3). The cnidarian TRAF2 and TRAF6 homologs were both highly efficient in inducing NF-κB in a human cellular background. In contrast to what would have been expected if a *Nematostella* type 1 paracaspase would have recruited one of the *Nematostella* TRAF homologs, no synergistic induction of NF-κB could be seen. This indicates that the evolution of type 1 paracaspases as NF-κB inducing scaffold proteins by recruitment of TRAF6 occurred later.

Conservation and co-evolution of the CBM complex

Previous studies has shown that the MALT1-like activities are conserved at least as far back as the last common ancestor of the three vertebrate type 1 paracaspase paralogs (Hulpiau et al. 2015). Similarly, also Bcl10 has been shown to be functionally conserved as far back as zebrafish (Mazzone et al. 2015). We also know that the upstream interaction to CARMA proteins is conserved at least as far back as zebrafish (Mazzone et al. 2015). We have now shown that Bcl10 and MALT1-like activities from type 1 paracaspases are considerably older, most likely preceding the Cambrian explosion (Dunn et al. 2014). The observation that invertebrate type 1 paracaspases from organisms that also contain Bcl10 are more similar to the vertebrate paracaspases provides a new interesting perspective on the functional evolution of MALT1. CARMA proteins are unique to vertebrates, but the conserved CARD-coiled-coil (CC) domain can be found in some invertebrates. Intriguingly, also these CARMA/CARD9-related CARD-CC domain proteins show a phylogenetic distribution which is similar to Bcl10 (Figure 4A), indicating that the entire CARD-CC/Bcl10/MALT1-like paracaspase (CBM) complex is co-evolving (Figure 5A) and that species with Bcl10-independent type 1 paracaspases rely on a completely independent activation mechanism. The placement of CARD14 (CARMA2) at the base of the CARMA/CARD9 proteins found in vertebrates based on the CARD domain phylogeny (Figure 4A) is consistent with phylogenies made with the MAGUK domain (de Mendoza et al. 2010), indicating that CARD14 might be the ancestral CARMA in vertebrates. In order to functionally verify the conservation of an upstream CARD-CC interaction with the Bcl10/paracaspase complex, we co-expressed either human CARD9 or *Nematostella* CARD-CC together with human MALT1 (Figure 4B). Also the cnidarian CARD-CC could induce a MALT1-dependent NF-κB induction, and consistent with previous observations (Afonina et al. 2016) is overexpression-induced NF-κB activation from CARD9 and CARD-CC very low. A likely evolutionary scenario for the CARMA proteins is that a CARD9-like CARD-CC got fused with a ZO-1/Dlg5-like MAGUK protein upstream of the PDZ domain early in the jawed vertebrate evolution. Interestingly, the presence of 3 CARMA paralogs and 3 type 1 paracaspase paralogs in the vertebrate lineage both seem to have arisen in the last common ancestor of jawed vertebrates, which coincides with the evolution of the vertebrate adaptive immune system (Rast and Buckley 2013). Lampreys only seem to have a single ancestral CARD-CC (Figure 4A) and a single type 1 paracaspase PCASP3 ortholog which seems to be the parent of the PCASP3 and PCASP(1/2) branches in jawed vertebrates (Figure 1B). Surprisingly, the supposedly ancestral CARD-CC in lampreys is clustering closer to CARD11 than CARD14. Taken together, we can however conclude that the CBM complex components seem to be evolutionary linked (Figure 5A) and functionally interacting ever since the last common ancestor of the planulozoans.

ITAM receptors and Syk : a potential original pathway for the CBM complex

Given the CARD9-like domain organization of the invertebrate CARD-CC homologs, it is tempting to speculate that the original role of the CBM complex was in the evolutionary conserved C-type lectin signaling pathway (Sattler et al. 2012; Drummond and Lionakis 2016). CARD9 is critical for immunity against fungal infections in humans (Alves de Medeiros et al. 2016). Interestingly, a NCBI BLASTP survey of invertebrate Dectin-1 C-lectin domain homologs finds back top-scoring hits from mollusks and cnidaria but not the much better characterized arthropod and nematode genomes (Pees et al. 2016), which is similar to previous observations (Wood-Charlson and Weis 2009). C-type lectins are already associated to innate immunity in mollusks (Li et al. 2015) and cnidaria (Vidal-Dupiol et al. 2009). Human Dectin-1 signal to the CARD9/Bcl10/MALT1 complex via the tyrosine kinase Syk and PKCδ. The top invertebrate Syk/Zap70 BLASTP hits also correlate with the presence of Bcl10/CARD-CC, where especially the N-terminal sequence of Syk was specific for those organisms (Figure 4C). This is in agreement with earlier observations of a loss of the Syk kinase during metazoan evolution that were made when much less sequence information was available (Steele et al. 1999). Strikingly, the pattern Syk-containing organisms is largely overlapping with organisms containing Bcl10 and CARD-CC homologs (Figure 5A). BLASTP with the 200 first residues of Syk or Zap70 made the CARD-CC/Bcl10-correlated phylogenetic distribution even clearer with deuterostome, mollusk and cnidarian proteins among the top hits. The N-terminal SH2 domains in Syk and Zap70 are critical for interaction with upstream ITAM domain containing receptors (Flaswinkel et al. 1995; Mócsai et al. 2010). The phylogenetic distribution of the SH2 domains in the tyrosine kinase Syk could be linked to the CBM complex evolution, which would indicate ITAM containing upstream receptors linked to the CBM complex (Figure 5B). There is no sequence hit of the N-terminal ITAM - containing intracellular domain of Dectin-1 in mollusks or cnidarian transmembrane C-type lectins and there is not yet true proof of a C-lectin receptor /Syk pathway in invertebrates. The ITAM - dependent signaling in those organisms could however be mediated by another class of receptors, as suggested for lamprey (Liu et al. 2015). In contrast to Syk, PKCδ homologs could be found in a wide range of invertebrates reflecting its importance in many alternative pathways. If the Syk/CBM pathway is shown to be conserved, further insight on the biology and regulation of the CBM complex would not only benefit biomedical research against (auto)immune diseases and cancer, but could also impact a wide range of other areas such as mollusk (aqua)culture and environmentally important challenges like the host immunity component of coral bleaching (Vidal-Dupiol et al. 2009; Bosch et al. 2014).

Future challenges

We still don't know how far back that MALT1-like activities such as TRAF6 interaction and NF-κB induction, protease activity and specificity are conserved. With the observation that mollusk paracaspases have conserved protease activity and specificity, but fail to induce NF-κB in a human cellular background, we are starting to unravel the sequence of evolutionary events leading to the current MALT1 activities in humans. It appears like the protease activity and substrate specificity precedes the evolution of the TRAF6 binding motifs in vertebrate paracaspases. A major future challenge will be to collect and functionally evaluate more invertebrate type 1 paracaspase, Bcl10 and CARD-CC homologs to verify the proposed correlation of a CARD-CC/Bcl10-dependent ancestral type 1 paracaspase paralog with MALT1-like activity and to model the evolution of the MALT1-Bcl10 interaction. There are several aspects that are yet not clear, for example can no Bcl10 or CARD-CC homolog currently be found in lancelets, which clearly have a PCASP3 ortholog (Hulpiau et al. 2015). The limited number of invertebrate true Bcl10 homologs that can be identified in public sequence data is currently a clear limitation for further analysis. CRADD homologs often are picked up as false positives in distant species since they contain a CARD domain that is very similar to Bcl10 (Lin et al. 2012; Qiao et al. 2014). The current model proposes an ancient parallel evolution of a Bcl10-dependent and a Bcl10-independent paracaspase (Figure 6). An alternative scenario is that Bcl10-independence has evolved several times independently. In order to further clarify this, more invertebrate sequences from informative phyla are needed (GIGA community of scientists 2014). Several proteins associated to MALT1 in humans are conserved as far back as cnidarians, such as CARMA/CARD9, Bcl10, TRAF6, TRAF2 and CYLD (Hulpiau et al. 2015), and we have now shown that they are functionally conserved in a human cellular environment. It would be very interesting to investigate the functional properties of paracaspases from species closely related to the jawed vertebrates such as lampreys and lancelets to identify when type 1 paracaspases evolved into NF-κB-inducing scaffold proteins. On the other hand, investigating early-diverging biological model systems such as the cnidarians for protein interactions and signal transduction mechanisms could further pin-point the original and most conserved functions in a native context. The anemone cnidarian model organisms *Nematostella vectensis* and *Aiptasia* might however not be the best choices since they express a short form of CYLD and do not have one of the typical cnidarian type 1 paracaspase paralogs found in hydra and corals (PCASP-t1C, Figure 1B). It is possible that the type 1 paracaspase that is missing in anemones has more MALT1-like characteristics. Furthermore, corals (e.g. *Acropora digitifera*) have been found to have a massively expanded immune repertoire compared to *Nematostella* (Shinzato et al. 2011; Quistad et al. 2014). Another highly interesting model organism to study would be the nematode model organism *C. elegans* to specifically investigate the CARD-CC/Bcl10- and NF-κB independent functions of type 1 paracaspases in bilaterans, which could give important clues to yet-undiscovered functions of human MALT1.

Materials & Methods

Sequences of type 1 paracaspases, Bcl10 and CARD-CC homologs

Protein sequences of type 1 paracaspase, Bcl10 and CARMA/CARD9 homologs were retrieved from NCBI (https://www.ncbi.nlm.nih.gov), Ensembl (http://metazoa.ensembl.org), JGI (http://genome.jgi.doe.gov/), OIST marine genomics (http://marinegenomics.oist.jp) (Shinzato et al. 2011) (Luo et al. 2015) (Simakov et al. 2015) , ReefGenomics (http://reefgenomics.org/)(Baumgarten et al. 2015) and ICMB (https://imcb.a-star.edu.sg) (Mehta et al. 2013; Venkatesh et al. 2014) using BLASTP (Johnson et al. 2008). All sequences used in the analyses can be found in supplemental material.

Sequence alignment and phylogenetic analysis

Sequence alignment was performed on the full sequence, using the different alignment algorithms Clustal Omega (Sievers and Higgins 2014), MUSCLE (http://www.drive5.com/muscle/) (Edgar 2004), and T-coffee (http://www.tcoffee.org/) (Notredame et al. 2000). Phylogenetic analysis was performed with PhyML (http://atgc_montpellier.fr/phyml/) (Guindon et al. 2009) and MrBayes (http://mrbayes.sourceforge.net/) (Ronquist and Huelsenbeck 2003) methods. Both alignments and phylogenetic analyses were performed using UGENE (http://ugene.net/) (Okonechnikov et al. 2012) on Arch (http://www.archlinux.org) Linux (Torvalds 1999). For the figures, one of the most representative trees (alignment+phylogenetic analysis) was selected. For independent replication of the results, all sequences used in the phylogenetic analysis are available in the supplemental data. Metadata by coloring the branches was manually added along with manual adjustment of line thickness using inkscape (https://inkscape.org). The type 1 paracaspase nematode/arthropod branch was also for aesthetic reasons manually rotated in the scalable vector graphics (svg) file without changing any branch lengths in order to avoid overlapping branches.

Cloning of invertebrate homologs

Plasmids of the cloned genes were deposited in the BCCM/LMBP plasmid collection along with detailed descriptions of cloning strategy and plasmid sequence (http://bccm.belspo.be/about-us/bccm-lmbp). The starlet sea anemone (*Nematostella vectensis)* type 1 paracaspase paralog “A” (LMBP: 9589) and zebrafish PCASP3 (LMBP: 9573) were cloned previously (Hulpiau et al. 2015). The *Nematostella* type 1 paracaspase paralogs “A” (LMBP: 9636) and “B” (LMBP: 9825) and pacific oyster (*Crassostrea gigas*, LMBP: 9826) were cloned behind the human ETV6 HLH domain for dimerization-induced activation as described previously (Malinverni et al. 2010; Baens et al. 2014; Hulpiau et al. 2015). Human (LMBP: 9637), zebrafish (LMBP: 9665), pacific oyster (LMBP: 9666) and *Nematostella* (LMBP: 9822) Bcl10 were cloned in the pCAGGS vector with an N-terminal E-tag. *Nematostella* CYLD (LMBP : 9900) was also cloned in pCAGGS with an N-terminal E-tag. The *Nematostella* homologs of CARD-CC (LMBP: 9854) TRAF6 (LMBP: 9855) and TRAF2 (LMBP: 9856) in a pCDNA3 vector with N-terminal Flag tag. For further specific cloning purposes, human CARD9 (LMBP: 9877), Bcl10 (LMBP: 9872), MALT1 (LMBP : 9104, 9105) and *Nematostella* CARD-CC (LMBP: 9873), Bcl10 (LMBP: 9874), PCASP-t1A (LMBP : 9875) and PCASP-t1B (LMBP : 9876) were cloned into gateway-compatible pENTR-vectors.

Cell culture, transfection and expression analysis

MALT1 KO HEK293T cells (clone #36) (Hulpiau et al. 2015) were grown under standard conditions (DMEM, 10% FCS, 5% CO_2, 37 ^oC) and transfected with the calcium phosphate method (Anon 2005). For evaluation of the conservation of cleavage activity, the HLH-fused paracaspase constructs were co-transfected with wild-type CYLD (LMBP: 6613) or the uncleavable CYLD-R324A (LMBP: 6645) mutant. Cells transfected for cleavage activity evaluations were lysed directly in Laemmli buffer (0.1% 2-Mercaptoethanol, 5ppm Bromophenol blue, 10% Glycerol, 2% SDS, 63 mM Tris-HCl (pH 6.8)). For evalutation of conservation of NF-κB induction, the HLH paracaspase fusions were co-transfected with a NF-κB luciferase reporter (LMBP: 3249) and actin promoter-driven β-galactosidase (LMBP: 4341) as transfection control. The cells used for luciferase analysis were washed with 1XPBS and lysed in luciferase lysis buffer (25mM Tris pH7.8, 2mM DTT, 2mM CDTA, 10% glycerol, 1% Triton X-100). For the colorimetric determination (at 595nm) of β-galactosidase activity, chlorophenol red-β-D-galactopyranoside (CPRG) (Roche diagnostics) was used as a substrate. The luciferase activity was measured by using beetle luciferin (Promega) as a substrate and the luminescence was measured with the GloMax® 96 Microplate Luminometer (Promega). Luciferase data processing and calculation of 95% confidence intervals (Student’s t-distribution (Student 1908)) was done in LibreOffice (www.libreoffice.org) Calc, a fork from OpenOffice (Gamalielsson and Lundell 2014). For evaluation of the functional conservation of the Bcl10 homologs, the Bcl10 clones were co-transfected with the NF-κB luciferase reporter and β-galactosidase in the MALT1 KO HEK293T cells with or without reconstitution with human MALT1 (LMBP: 5536). The human CARD9 (LMBP: 9609) was used as control for evaluations of the functional conservation of CARD-CC proteins. Detection of cleaved CYLD was done with the E10 antibody (Santa Cruz Biotechnology) recognizing the C-terminal 70kDa cleavage band or anti-E-tag (ab66152, Abcam) recognizing the 40kDa N-terminal cleavage band. Expression of the fused paracaspases was determined with anti-Flag (F-3165, Sigma). Human MALT1 was detected by the EP603Y monoclonal rat

antibody (Abcam) and the E-tagged Bcl10 clones with anti-E-tag. All western blots were developed on an Odyssey scanner (LI-COR).

Yeast-2-hybrid assay

Human MALT1 (LMBP: 9880, 9899), Bcl10 (LMBP : 9879, 9885), CARD9 (LMBP: 9878, 9884) and Nematostella PCASP-t1A (LMBP: 9898) PCASP-t1B (LMBP: 9883, 9888), Bcl10 (LMBP : 9882, 9887) and CARD-CC (LMBP: 9881, 9886) were cloned into the pdGADT7 and pdGBKT7 vectors by Gateway LR reaction. The ENTR vectors were linearized to enable cloning into the kanamycin-resistant destination vector without background contamination. The Matchmaker Gold Yeast Two-Hybrid System (Clontech) was used with the Y2H Gold yeast strain to investigate protein-protein interactions. A pre-culture was made the day before transformation, by inoculating about 10 colonies of Y2H gold strain in 5 ml YPDA medium and growing it for about 4 h in a 30°C shaking incubator. The pre-culture was transferred to 35 ml YPDA and grown overnight in a 30°C shaking incubator. On the day of transformation, the overnight culture was diluted to an OD_{600} of 0.2 in YPDA (depending on the number of transformations, 10 ml YPDA/transformation) and grown in a 30°C shaking incubator until an OD_{600} of 0.6–0.8. After a 5 min centrifugation step at 2100 rpm 23 °C, the yeast pellet was resuspended in 10 ml Milli-Q water and centrifuged again for 5 min. After resuspending the pellet in 1x TE/LiAc, 100 µl of competent cells were mixed with 100 µg denatured salmon sperm DNA, 1 µg bait plasmid, 1 µg prey plasmid and 600 µl fresh PEG400/LiAc. The yeast-DNA mixtures were incubated in a 30°C shaking incubator for 30 min. The yeast cells were transformed via heat-shock at 42°C for 15 min. After a 1-min incubation on ice and a 30-sec centrifugation step, the pellet was resuspended in 1x TE and plated on minimal synthetic drop-out medium (SD) lacking leucine and tryptophan (SD -Leu/-Trp). After 4 days of incubation at 30°C, colonies were picked and incubated overnight in 200 µl SD/-Leu/-Trp medium in a 96-well plate. Transformed yeast cells were grown overnight in a 30°C incubator. Cultures were then stamped on SD/-Leu/-Trp and SD/-Leu/-Trp/-His/-Ade/+X-α-gal (40 µg/mL 5-bromo-4-chloro-3 indolyl-b-D-galactopyranoside) plates using an iron 96-well stamp and incubated for 3-7 days at 30°C until blue colonies were visible.

In situ expression analysis in Nematostella

As RNA probe templates, pDEST12.2 clones of Nematostella CARD-CC (LMBP:), Bcl10 (LMBP:), PCASP-t1A (LMBP:) and PCASP-t1B (LMBP:) were generated by Gateway LR reaction. SP6 RNA polymerase () was used to generate labeled RNA probes. Fixed *N. vectensis* embryos were transferred into wells and rehydrated with 60% methanol / 40% PBS with 0.1% Tween 20 (PBSTw), 40% methanol / 60% PBSTw and four times with 100% PBSTw. The samples were then digested with 10 µg/ml Proteinase K (prepared in PBSTw) for 20 min. The reaction was stopped by two washes with 4 mg/ml glycine. The embryos were washed first with 1% triethanolamine (v/v in PBSTw), two times with 1% triethanolamine / 3 µl acetic anhydride and then two times with 1% triethanolamine / 6 µl acetic anhydride. After two washes with PBSTw, the embryos were refixed in 3.7% paraformaldehyde (v/v in PBSTw) for one hour and washed five times with PBSTw. Samples were prehybridized in 50% PBSTw / 50% Hybridization buffer (Hybe) (50% formamide, 5X SSC, 50 µg/ml heparin, 0.1% Tween 20 (v/v), 1% SDS (v/v) 100 µg/ml SS DNA and DEPC water) for 10 min, 100% Hybe buffer for 10 min and 100% Hybe buffer overnight at 60°C. Labelled RNA probes were diluted to 0.5 ng/µl Hybe buffer and denatured at 85°C for 10 min. Hybe buffer was removed from the embryos and for each reaction 250-300 µl working stock probe was added into the *in situ* plate. The sieves with embryos were transferred to the in situ plate and sealed to prevent evaporation. The embryos were then incubated at 60°C for 48-72 hours. The sieves were transferred to a clean rack filled with fresh preheated (to the hybridization temperature) Hybe buffer and incubated at 60°C for 10 min. Then the samples were washed with 100% Hybe buffer and incubated at the hybridization temperature for 40 min. The embryos were washed at hybridization temperature for 30 min; once with 75% Hybe / 25% 2X SSCT (pH 7.0, 0.3 M sodium citrate, 3 M NaCl and 0.1% (v/v) Tween 20), once with 50% Hybe / 50% 2X SSCT, once with 25% Hybe / 75% 2X SSCT, once with 2X SSCT and finally three times with 0.05X SSCT. Prior to the blocking step, the samples were washed three times with 100% PBSTw (each 10 min) at room temperature. To decrease the unspecific background, the samples were blocked in Roche blocking reagent (supplemented with 1% (w/v) 1X maleic acid) for one hour at room temperature. The embryos were then incubated with antibody solution (Roche anti-digoxigenin-AP (alkaline phosphatase) diluted 1/2000 in blocking buffer) at 4°C overnight. The sieves were rinsed with blocking buffer and washed 10 times with 100% PBSTw (each 15 min). The embryos were developed in AP substrate solution (5 M NaCl, 1 M $MgCl_2$, 1 M Tris pH 9.5 and 0.1% (v/v) Tween 20) at room temperature. Color development was checked every 10 min for 2 hours and AP substrate solution was replaced if an extended developing period was required. Once the probe development reached the desired level, the reaction was stopped by washing with 100% PBSTw. Next, the samples were washed with 100% ethanol for 1 hour and rinsed several times with 100% PBSTw. Finally, the specimens were washed with 85% glycerol (in PBSTw) at 4°C overnight and embedded to microscope slides.

Supplemental material

Supplemental text 1 : FASTA sequences of type 1 paracaspases used in phylogeny
Supplemental text 2 : FASTA sequences of Bcl10 homologs used in phylogeny

Supplemental text 3 : FASTA sequences of CARMA/CARD9 homologs used in phylogeny

Supplemental text 4 : FASTA sequences of Zap70/Syk homologs

References

Afonina IS, Van Nuffel E, Baudelet G, Driege Y, Kreike M, Staal J, Beyaert R. 2016. The paracaspase MALT1 mediates CARD14-induced signaling in keratinocytes. EMBO Rep. [Internet]. Available from: http://embor.embopress.org/content/early/2016/04/25/embr.201642109.abstract

Alves de Medeiros AK, Lodewick E, Bogaert DJA, Haerynck F, Van Daele S, Lambrecht B, Bosma S, Vanderdonckt L, Lortholary O, Migaud M, et al. 2016. Chronic and Invasive Fungal Infections in a Family with CARD9 Deficiency. J. Clin. Immunol. 36:204–209.

Anon. 2005. Calcium phosphate–mediated transfection of eukaryotic cells. Nat. Methods 2:319–320.

Baens M, Bonsignore L, Somers R, Vanderheydt C, Weeks SD, Gunnarsson J, Nilsson E, Roth RG, Thome M, Marynen P. 2014. MALT1 auto-proteolysis is essential for NF-κB-dependent gene transcription in activated lymphocytes. PloS One 9:e103774.

Baumgarten S, Simakov O, Esherick LY, Liew YJ, Lehnert EM, Michell CT, Li Y, Hambleton EA, Guse A, Oates ME, et al. 2015. The genome of Aiptasia, a sea anemone model for coral symbiosis. Proc. Natl. Acad. Sci. 112:11893–11898.

Bognar MK, Vincendeau M, Erdmann T, Seeholzer T, Grau M, Linnemann JR, Ruland J, Scheel CH, Lenz P, Ott G, et al. 2016. Oncogenic CARMA1 couples NF-κB and β-catenin signaling in diffuse large B-cell lymphomas. Oncogene.

Bosch TCG, Adamska M, Augustin R, Domazet-Loso T, Foret S, Fraune S, Funayama N, Grasis J, Hamada M, Hatta M, et al. 2014. How do environmental factors influence life cycles and development? An experimental framework for early-diverging metazoans. BioEssays News Rev. Mol. Cell. Dev. Biol. 36:1185–1194.

C. elegans Deletion Mutant Consortium. 2012. large-scale screening for targeted knockouts in the Caenorhabditis elegans genome. G3 Bethesda Md 2:1415–1425.

Che T, You Y, Wang D, Tanner MJ, Dixit VM, Lin X. 2004. MALT1/paracaspase is a signaling component downstream of CARMA1 and mediates T cell receptor-induced NF-kappaB activation. J. Biol. Chem. 279:15870–15876.

Coornaert B, Baens M, Heyninck K, Bekaert T, Haegman M, Staal J, Sun L, Chen ZJ, Marynen P, Beyaert R. 2008. T cell antigen receptor stimulation induces MALT1 paracaspase-mediated cleavage of the NF-kappaB inhibitor A20. Nat Immunol 9:263–271.

Darling JA, Reitzel AR, Burton PM, Mazza ME, Ryan JF, Sullivan JC, Finnerty JR. 2005. Rising starlet: the starlet sea anemone, Nematostella vectensis. BioEssays News Rev. Mol. Cell. Dev. Biol. 27:211–221.

Demeyer A, Staal J, Beyaert R. 2016. Targeting MALT1 Proteolytic Activity in Immunity, Inflammation and Disease: Good or Bad? Trends Mol. Med.

Dierlamm J, Baens M, Wlodarska I, Stefanova-Ouzounova M, Hernandez JM, Hossfeld DK, Wolf-Peeters CD, Hagemeijer A, Berghe HV den, Marynen P. 1999. The Apoptosis Inhibitor Gene API2 and a Novel 18q Gene,MLT, Are Recurrently Rearranged in the t(11;18)(q21;q21) Associated With Mucosa-Associated Lymphoid Tissue Lymphomas. Blood 93:3601–3609.

Douanne T, Gavard J, Bidère N. 2016. The paracaspase MALT1 cleaves the LUBAC subunit HOIL1 during antigen receptor signaling. J. Cell Sci.

Drummond RA, Lionakis MS. 2016. Mechanistic Insights into the Role of C-Type Lectin Receptor/CARD9 Signaling in Human Antifungal Immunity. Front. Cell. Infect. Microbiol. 6:39.

Dunn CW, Giribet G, Edgecombe GD, Hejnol A. 2014. Animal Phylogeny and Its Evolutionary Implications. Annu. Rev. Ecol. Evol. Syst. 45:371–395.

Edgar RC. 2004. MUSCLE: multiple sequence alignment with high accuracy and high throughput. Nucleic Acids Res. 32:1792–1797.

Elton L, Carpentier I, Staal J, Driege Y, Haegman M, Beyaert R. 2015. MALT1 cleaves the E3 ubiquitin ligase HOIL-1 in activated T cells, generating a dominant negative inhibitor of LUBAC-induced NF-κB signaling. FEBS J.

Ferch U, zum Büschenfelde CM, Gewies A, Wegener E, Rauser S, Peschel C, Krappmann D, Ruland J. 2007. MALT1 directs B cell receptor-induced canonical nuclear factor-kappaB signaling selectively to the c-Rel subunit. Nat. Immunol. 8:984–991.

Flaswinkel H, Barner M, Reth M. 1995. The tyrosine activation motif as a target of protein tyrosine kinases and SH2 domains. Semin. Immunol. 7:21–27.

Fontan L, Yang C, Kabaleeswaran V, Volpon L, Osborne MJ, Beltran E, Garcia M, Cerchietti L, Shaknovich R, Yang SN, et al. 2012. MALT1 small molecule inhibitors specifically suppress ABC-DLBCL in vitro and in vivo. Cancer Cell 22:812–824.

Gamalielsson J, Lundell B. 2014. Sustainability of Open Source software communities beyond a fork: How and why has the LibreOffice project evolved? J. Syst. Softw. 89:128–145.

GIGA community of scientists. 2014. The Global Invertebrate Genomics Alliance (GIGA): Developing Community Resources to Study Diverse Invertebrate Genomes. J. Hered. 105:1–18.

Gringhuis SI, Wevers BA, Kaptein TM, van Capel TMM, Theelen B, Boekhout T, de Jong EC, Geijtenbeek TBH. 2011. Selective C-Rel activation via Malt1 controls anti-fungal T(H)-17 immunity by dectin-1 and dectin-2. PLoS Pathog. 7:e1001259.

Gross O, Gewies A, Finger K, Schäfer M, Sparwasser T, Peschel C, Förster I, Ruland J. 2006. Card9 controls a non-TLR signalling pathway for innate anti-fungal immunity. Nature 442:651–656.

Guindon S, Delsuc F, Dufayard J-F, Gascuel O. 2009. Estimating maximum likelihood phylogenies with PhyML. Methods Mol. Biol. Clifton NJ 537:113–137.

Hachmann J, Snipas SJ, van Raam BJ, Cancino EM, Houlihan EJ, Poreba M, Kasperkiewicz P, Drag M, Salvesen GS. 2012. Mechanism and specificity of the human paracaspase MALT1. Biochem. J. 443:287–295.

Hailfinger S, Nogai H, Pelzer C, Jaworski M, Cabalzar K, Charton J-E, Guzzardi M, Décaillet C, Grau M, Dörken B, et al. 2011. Malt1-Dependent RelB Cleavage Promotes Canonical NF-κB Activation in Lymphocytes and Lymphoma Cell Lines. Proc. Natl. Acad. Sci. 108:14596–14601.

Hamilton KS, Phong B, Corey C, Cheng J, Gorentla B, Zhong X, Shiva S, Kane LP. 2014. T cell receptor-dependent activation of mTOR signaling in T cells is mediated by Carma1 and MALT1, but not Bcl10. Sci. Signal. 7:ra55.

Hopf TA, Schärfe CPI, Rodrigues JPGLM, Green AG, Kohlbacher O, Sander C, Bonvin AMJJ, Marks DS. 2014. Sequence co-evolution gives 3D contacts and structures of protein complexes. eLife 3.

Howes A, O'Sullivan PA, Breyer F, Ghose A, Cao L, Krappmann D, Bowcock AM, Ley SC. 2016. Psoriasis mutations disrupt CARD14 autoinhibition promoting BCL10-MALT1-dependent NF-κB activation. Biochem. J.

Hulpiau P, Driege Y, Staal J, Beyaert R. 2015. MALT1 is not alone after all: identification of novel paracaspases. Cell. Mol. Life Sci. CMLS.

Jeltsch KM, Hu D, Brenner S, Zöller J, Heinz GA, Nagel D, Vogel KU, Rehage N, Warth SC, Edelmann SL, et al. 2014. Cleavage of roquin and regnase-1 by the paracaspase MALT1 releases their cooperatively repressed targets to promote T(H)17 differentiation. Nat. Immunol. 15:1079–1089.

Johnson M, Zaretskaya I, Raytselis Y, Merezhuk Y, McGinnis S, Madden TL. 2008. NCBI BLAST: a better web interface. Nucleic Acids Res. 36:W5-9.

Klein T, Fung S-Y, Renner F, Blank MA, Dufour A, Kang S, Bolger-Munro M, Scurll JM, Priatel JJ, Schweigler P, et al. 2015. The paracaspase MALT1 cleaves HOIL1 reducing linear ubiquitination by LUBAC to dampen lymphocyte NF-κB signalling. Nat. Commun. 6:8777.

Knoll A, Walter M, Narbonne G, Christie-Blick N. 2006. The Ediacaran Period: a new addition to the geologic time scale. Lethaia 39:13–30.

Langel FD, Jain NA, Rossman JS, Kingeter LM, Kashyap AK, Schaefer BC. 2008. Multiple Protein Domains Mediate Interaction between Bcl10 and MALT1. J. Biol. Chem. 283:32419–32431.

Li H, Zhang H, Jiang S, Wang W, Xin L, Wang H, Wang L, Song L. 2015. A single-CRD C-type lectin from oyster Crassostrea gigas mediates immune recognition and pathogen elimination with a potential role in the activation of complement system. Fish Shellfish Immunol. 44:566–575.

Lin Q, Liu Y, Moore DJ, Elizer SK, Veach RA, Hawiger J, Ruley HE. 2012. Cutting edge: the "death" adaptor CRADD/RAIDD targets BCL10 and suppresses agonist-induced cytokine expression in T lymphocytes. J. Immunol. Baltim. Md 1950 188:2493–2497.

Liu C, Su P, Li R, Zhang Q, Zhu T, Liu X, Li Q. 2015. Molecular cloning, expression pattern, and molecular evolution of the spleen tyrosine kinase in lamprey, Lampetra japonica. Dev. Genes Evol. 225:113–120.

Long KA, Nossa CW, Sewell MA, Putnam NH, Ryan JF. 2016. Low coverage sequencing of three echinoderm genomes: the brittle star Ophionereis fasciata, the sea star Patiriella regularis, and the sea cucumber Australostichopus mollis. GigaScience 5:20.

Luo Y-J, Takeuchi T, Koyanagi R, Yamada L, Kanda M, Khalturina M, Fujie M, Yamasaki S, Endo K, Satoh N. 2015. The Lingula genome provides insights into brachiopod evolution and the origin of phosphate biomineralization. Nat. Commun. 6:8301.

Malinverni C, Unterreiner A, Staal J, Demeyer A, Galaup M, Luyten M, Beyaert R, Bornancin F. 2010. Cleavage by MALT1 induces cytosolic release of A20. Biochem. Biophys. Res. Commun. 400:543–547.

Mazzone P, Scudiero I, Ferravante A, Paolucci M, D'Andrea LE, Varricchio E, Telesio G, De Maio C, Pizzulo M, Zotti T, et al. 2015. Functional characterization of zebrafish (Danio rerio) Bcl10. PloS One 10:e0122365.

McAllister-Lucas LM, Ruland J, Siu K, Jin X, Gu S, Kim DSL, Kuffa P, Kohrt D, Mak TW, Nuñez G, et al. 2007. CARMA3/Bcl10/MALT1-dependent NF-kappaB activation mediates angiotensin II-responsive inflammatory signaling in nonimmune cells. Proc Natl Acad Sci U A 104:139–144.

Mehta TK, Ravi V, Yamasaki S, Lee AP, Lian MM, Tay B-H, Tohari S, Yanai S, Tay A, Brenner S, et al. 2013. Evidence for at least six Hox clusters in the Japanese lamprey (Lethenteron japonicum). Proc. Natl. Acad. Sci. 110:16044–16049.

de Mendoza A, Suga H, Ruiz-Trillo I. 2010. Evolution of the MAGUK protein gene family in premetazoan lineages. BMC Evol. Biol. 10:93.

Meyer E, Weis VM. 2012. Study of Cnidarian-Algal Symbiosis in the "Omics" Age. Biol. Bull. 223:44–65.

Mócsai A, Ruland J, Tybulewicz VLJ. 2010. The SYK tyrosine kinase: a crucial player in diverse biological functions. Nat. Rev. Immunol. 10:387–402.

Nie Z, Du M-Q, McAllister-Lucas LM, Lucas PC, Bailey NG, Hogaboam CM, Lim MS, Elenitoba-Johnson KSJ. 2015. Conversion of the LIMA1 tumour suppressor into an oncogenic LMO-like protein by API2-MALT1 in MALT lymphoma. Nat. Commun. 6:5908.

Noels H, van Loo G, Hagens S, Broeckx V, Beyaert R, Marynen P, Baens M. 2007. A Novel TRAF6 binding site in MALT1 defines distinct mechanisms of NF-kappaB activation by API2middle dotMALT1 fusions. J. Biol. Chem. 282:10180–10189.

Notredame C, Higgins DG, Heringa J. 2000. T-Coffee: A novel method for fast and accurate multiple sequence alignment. J. Mol. Biol. 302:205–217.

Okonechnikov K, Golosova O, Fursov M, UGENE team. 2012. Unipro UGENE: a unified bioinformatics toolkit. Bioinforma. Oxf. Engl. 28:1166–1167.

Pees B, Yang W, Zárate-Potes A, Schulenburg H, Dierking K. 2016. High Innate Immune Specificity through Diversified C-Type Lectin-Like Domain Proteins in Invertebrates. J. Innate Immun. 8:129–142.

Peterson KJ, Lyons JB, Nowak KS, Takacs CM, Wargo MJ, McPeek MA. 2004. Estimating metazoan divergence times with a molecular clock. Proc. Natl. Acad. Sci. U. S. A. 101:6536–6541.

Qiao H, Liu Y, Veach RA, Wylezinski L, Hawiger J. 2014. The adaptor CRADD/RAIDD controls activation of endothelial cells by proinflammatory stimuli. J. Biol. Chem. 289:21973–21983.

Quistad SD, Stotland A, Barott KL, Smurthwaite CA, Hilton BJ, Grasis JA, Wolkowicz R, Rohwer FL. 2014. Evolution of TNF-induced apoptosis reveals 550 My of functional conservation. Proc. Natl. Acad. Sci. U. S. A. 111:9567–9572.

Rast JP, Buckley KM. 2013. Lamprey immunity is far from primitive. Proc. Natl. Acad. Sci. 110:5746–5747.

Rebeaud F, Hailfinger S, Posevitz-Fejfar A, Tapernoux M, Moser R, Rueda D, Gaide O, Guzzardi M, Iancu EM, Rufer N, et al. 2008. The proteolytic activity of the paracaspase MALT1 is key in T cell activation. Nat Immunol 9:272–281.

Riviere G, Klopp C, Ibouniyamine N, Huvet A, Boudry P, Favrel P. 2015. GigaTON: an extensive publicly searchable database providing a new reference transcriptome in the pacific oyster Crassostrea gigas. BMC Bioinformatics 16:401.

Ronquist F, Huelsenbeck JP. 2003. MrBayes 3: Bayesian phylogenetic inference under mixed models. Bioinforma. Oxf. Engl. 19:1572–1574.

Ruefli-Brasse AA, French DM, Dixit VM. 2003. Regulation of NF-kappaB-dependent lymphocyte activation and development by paracaspase. Science 302:1581–1584.

Ruland J, Duncan GS, Wakeham A, Mak TW. 2003. Differential requirement for Malt1 in T and B cell antigen receptor signaling. Immunity 19:749–758.

Sakamaki K, Shimizu K, Iwata H, Imai K, Satou Y, Funayama N, Nozaki M, Yajima M, Nishimura O, Higuchi M, et al. 2014. The apoptotic initiator caspase-8: its functional ubiquity and genetic diversity during animal evolution. Mol. Biol. Evol. 31:3282–3301.

Salvesen GS, Hempel A, Coll NS. 2015. Protease signaling in animal and plant-regulated cell death. FEBS J.

Sattler S, Ghadially H, Hofer E. 2012. Evolution of the C-Type Lectin-Like Receptor Genes of the DECTIN-1 Cluster in the NK Gene Complex. Sci. World J. [Internet] 2012. Available from: http://www.ncbi.nlm.nih.gov/pmc/articles/PMC3322459/

Schmitt A, Grondona P, Maier T, Brändle M, Schönfeld C, Jäger G, Kosnopfel C, Eberle FC, Schittek B, Schulze-Osthoff K, et al. 2016. MALT1 Protease Activity Controls the Expression of Inflammatory Genes in Keratinocytes upon Zymosan Stimulation. J. Invest. Dermatol. 136:788–797.

Scudiero I, Vito P, Stilo R. 2013. The Three CARMA Sisters: So Different, So Similar. A Portrait of the Three CARMA Proteins and their Involvement in Human Disorders. J. Cell. Physiol.

Shinzato C, Shoguchi E, Kawashima T, Hamada M, Hisata K, Tanaka M, Fujie M, Fujiwara M, Koyanagi R, Ikuta T, et al. 2011. Using the Acropora digitifera genome to understand coral responses to environmental change. Nature 476:320–323.

Sievers F, Higgins DG. 2014. Clustal Omega, accurate alignment of very large numbers of sequences. Methods Mol. Biol. Clifton NJ 1079:105–116.

Simakov O, Kawashima T, Marlétaz F, Jenkins J, Koyanagi R, Mitros T, Hisata K, Bredeson J, Shoguchi E, Gyoja F, et al. 2015. Hemichordate genomes and deuterostome origins. Nature 527:459–465.

Staal J, Driege Y, Bekaert T, Demeyer A, Muyllaert D, Damme PV, Gevaert K, Beyaert R. 2011. T-cell receptor-induced JNK activation requires proteolytic inactivation of CYLD by MALT1. EMBO J. 30:1742–1752.

Steele RE, Stover NA, Sakaguchi M. 1999. Appearance and disappearance of Syk family protein-tyrosine kinase genes during metazoan evolution. Gene 239:91–97.

Student. 1908. The probable error of a mean. Biometrika 6:1–25.

Sullivan JC, Wolenski FS, Reitzel AM, French CE, Traylor-Knowles N, Gilmore TD, Finnerty JR. 2009. Two Alleles of NF-?B in the Sea Anemone Nematostella vectensis Are Widely Dispersed in Nature and Encode Proteins with Distinct Activities. PLoS ONE [Internet] 4. Available from: http://www.ncbi.nlm.nih.gov/pmc/articles/PMC2751831/

Torvalds L. 1999. The Linux Edge. Commun ACM 42:38–39.

Uehata T, Iwasaki H, Vandenbon A, Matsushita K, Hernandez-Cuellar E, Kuniyoshi K, Satoh T, Mino T, Suzuki Y, Standley DM, et al. 2013. Malt1-Induced Cleavage of Regnase-1 in CD4+ Helper T Cells Regulates Immune Activation. Cell 153:1036–1049.

Uren AG, O'Rourke K, Aravind LA, Pisabarro MT, Seshagiri S, Koonin EV, Dixit VM. 2000. Identification of paracaspases and metacaspases: two ancient families of caspase-like proteins, one of which plays a key role in MALT lymphoma. Mol Cell 6:961–967.

Venkatesh B, Lee AP, Ravi V, Maurya AK, Lian MM, Swann JB, Ohta Y, Flajnik MF, Sutoh Y, Kasahara M, et al. 2014. Elephant shark genome provides unique insights into gnathostome evolution. Nature 505:174–179.

Vidal-Dupiol J, Adjeroud M, Roger E, Foure L, Duval D, Mone Y, Ferrier-Pages C, Tambutte E, Tambutte S, Zoccola D, et al. 2009. Coral bleaching under thermal stress: putative involvement of host/symbiont recognition mechanisms. BMC Physiol. 9:14.

Wiesmann C, Leder L, Blank J, Bernardi A, Melkko S, Decock A, D'Arcy A, Villard F, Erbel P, Hughes N, et al. 2012. Structural Determinants of MALT1 Protease Activity. J. Mol. Biol. 419:4–21.

Woo H-N, Hong G-S, Jun J-I, Cho D-H, Choi H-W, Lee H-J, Chung C-W, Kim I-K, Jo D-G, Pyo J-O, et al. 2004. Inhibition of Bcl10-mediated activation of NF-kappa B by BinCARD, a Bcl10-interacting CARD protein. FEBS Lett. 578:239–244.

Wood-Charlson EM, Weis VM. 2009. The diversity of C-type lectins in the genome of a basal metazoan, Nematostella vectensis. Dev. Comp. Immunol. 33:881–889.

Yu JW, Jeffrey PD, Ha JY, Yang X, Shi Y. 2011. Crystal Structure of the Mucosa-Associated Lymphoid Tissue Lymphoma Translocation 1 (MALT1) Paracaspase Region. Proc. Natl. Acad. Sci. 108:21004–21009.

Zhang G, Fang X, Guo X, Li L, Luo R, Xu F, Yang P, Zhang L, Wang X, Qi H, et al. 2012. The oyster genome reveals stress adaptation and complexity of shell formation. Nature 490:49–54.

Figure 1
Phylogeny of Bcl10 and type 1 paracaspases

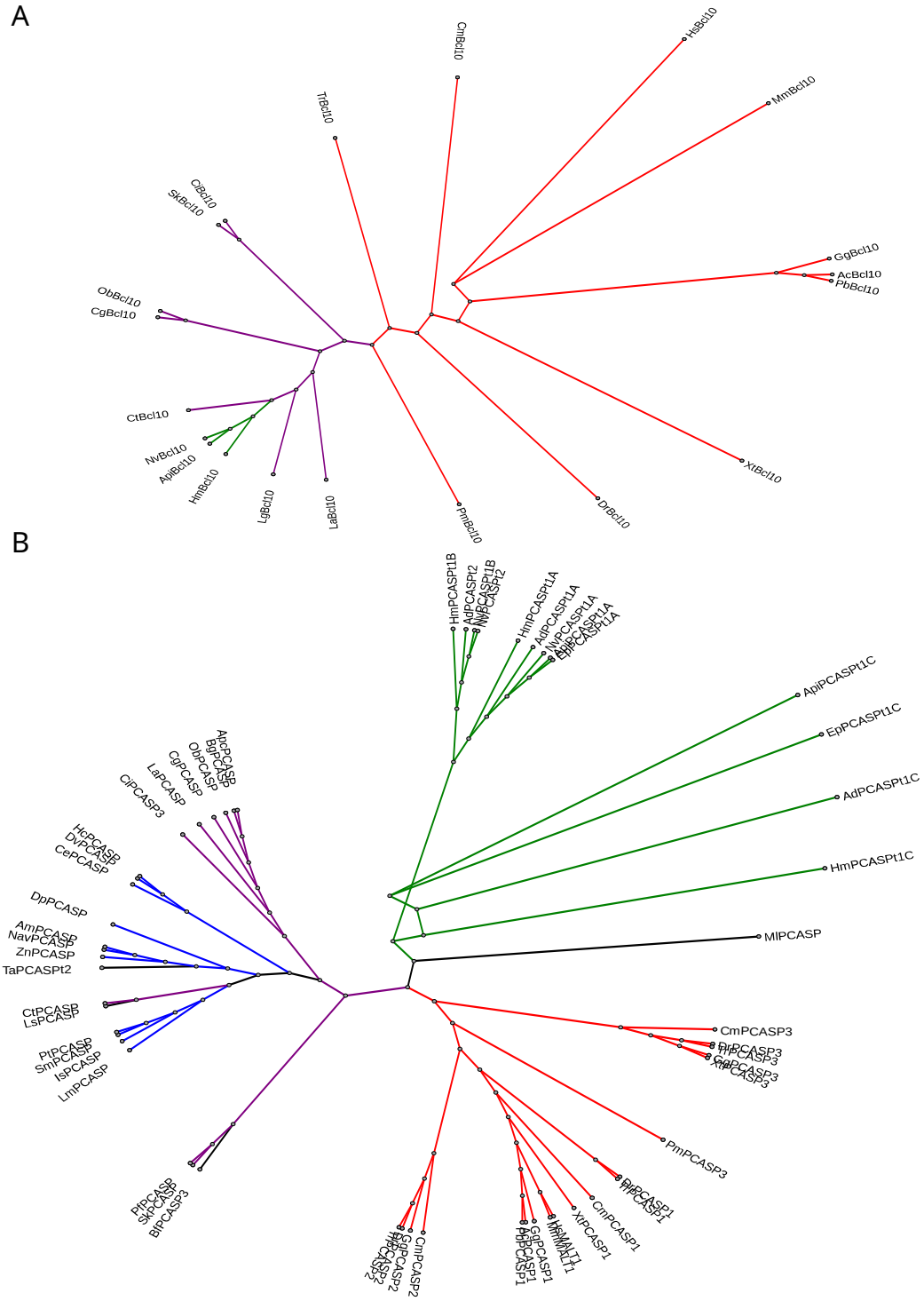

Species key: Vertebrates: Hs=Human, Mm=mouse, Gg=Chicken, Pb=Python, Ac=anole lizard Xt=African clawed frog, Dr=Zebrafish, Tr=Fugu, Cm=Elephant shark, Pm=Sea lamprey. Tunicates: Ci=Vase tunicate Lancelets: Bf=Florida lancelet. Hemichordates: Sk=Acorn worm Pf=Hawaiian acorn worm mollusks: Cg=Pacifc oyster, Lg=Limpet, Ob=Califonia two-spot octopus Brachiopods: La=*L. anatina* Annelids: Ct=polychaete worm Arthropods: Dp=Water flea, Am=Honey bee, Nav=jewel wasp, Sm=African social velvet spider, Pt=common house spider, Is=Fire ant, Lm=Horseshoe crab, Ls=salmon louse, Zn=termite Nematodes: Ce, Dr, Hc Cnidaria: Nv=Starlet sea anemone, Api=sea anemone, Ep=sea anemone, Hm=Hydra, Ad=Stag horn coral, Out groups: Ctenophora: Ml=comb jelly, Placozoa: Ta=*T. adherens*.
Vertebrates highlighted with red branches, bilateran invertebrate species with Bcl10 with purple branches, cnidaria with green and species from phyla completely lacking Bcl10 (e.g. arthropods, nematodes) with blue.
A) A representative phylogenetic tree of Bcl10 (MUSCLE + PhyML).
B) A representative phylogenetic tree (MUSCLE + PhyML) of the type 1 paracaspases:

Figure 2

Functional conservation of invertebrate paracaspase and Bcl10

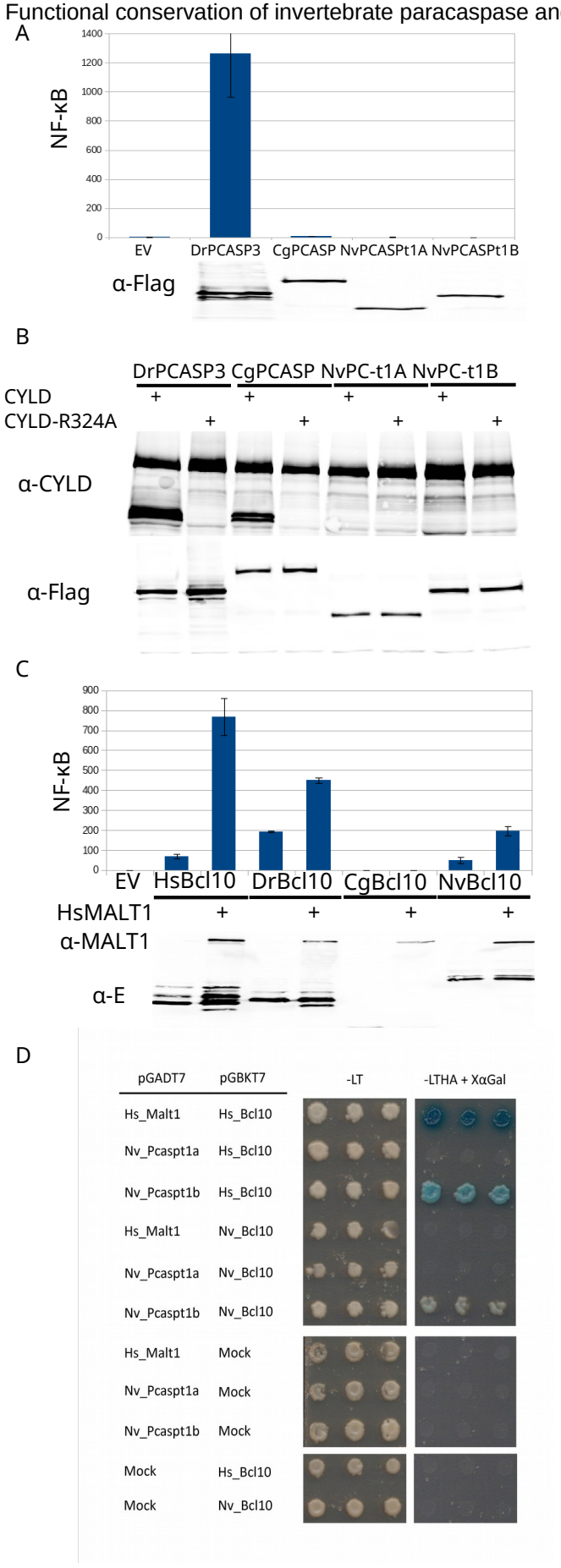

A) NF-κB induction by activated HLH-paracaspase fusions expressed in MALT1 KO HEK293T cells. Luciferase values are normalized against β-galactosidase and expressed as fold induction compared to samples not expressing a HLH-paracaspase fusion (EV). Error bars represent 95% confidence intervals. **B**)

CYLD cleavage by activated HLH-paracaspase fusions. Human CYLD is specifically cleaved by vertebrate paracaspases after residue R324, resulting in a 70kDa C-terminal fragment and a 40kDa N-terminal fragment. Cleavage of WT CYLD but failure to cleave the R324A mutant indicate a conserved substrate specificity. **C**) Human MALT1-dependent NF-κB induction by different Bcl10 homologs. The different Bcl10 homologs were expressed in MALT1 KO HEK293T cells. Bcl10 induces NF-κB via MALT1, which is illustrated by the increase of luciferase activity when the cells are reconstituted with human MALT1. Luciferase values are normalized against β-galactosidase and expressed as fold induction compared to samples not expressing Bcl10 (EV). Error bars represent 95% confidence intervals (Student's t-distribution). All experiments were repeated at least twice. **D)** Yeast-2-hybrid demonstrating conserved interaction between cnidarian and bilateran Bcl10 and type 1 paracaspase. One cnidarian type 1 paracaspase paralog is not binding Bcl10.

Figure 3
Functional conservation of cnidarian TRAF6 and TRAF2

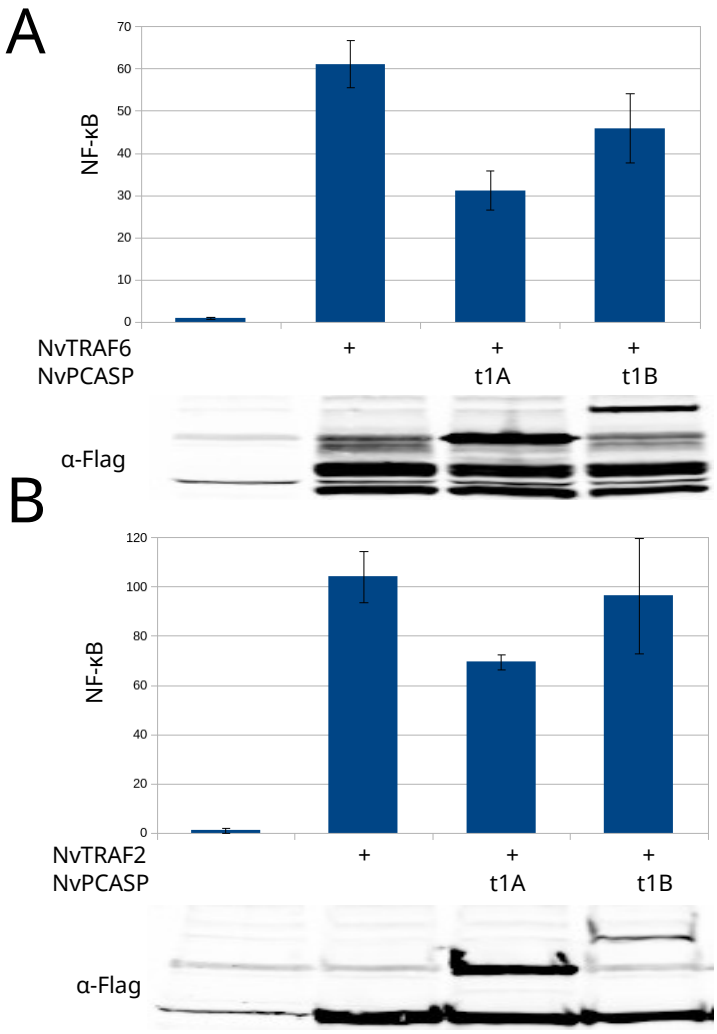

A) Functional conservation of TRAF6,
B) Functional conservation of TRAF2

Figure 4
Evolution of CARD9/CARMA-homologs and upstream Syk

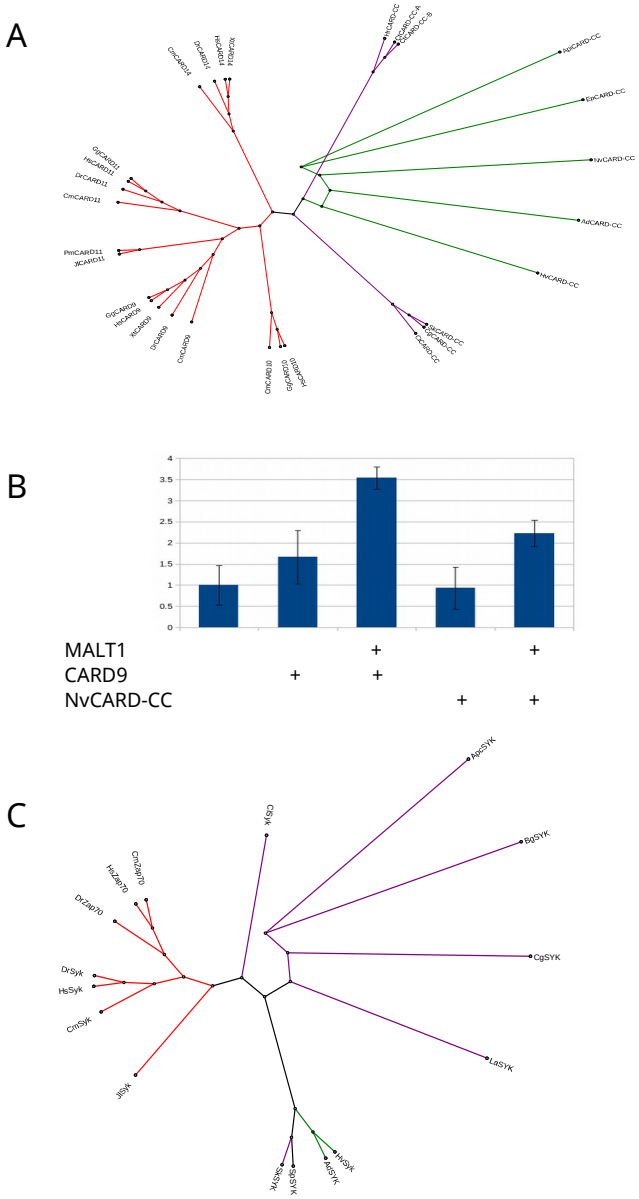

Species key: Vertebrates: Hs=Human, Gg=Chicken, Xt=African clawed frog, Dr=Zebrafish, Cm=Elephant shark, Pm=Sea lamprey, Jl=Japanese lamprey Tunicates: Ci=vase tunicate Hemichordates: Sk=Acorn worm mollusks: Cg=Pacifc oyster Annelids: Ct=polychaete worm, Hr=leech Cnidaria: Nv=Starlet sea anemone, Hm=Hydra, Ep=Sea anemone. Red branches highlight vertebrate sequences, green branches cnidaria and purple branches bilateran invertebrates with Bcl10.

A) A representrative tree (MUSCLE+PhyML) showing the relationships between CARD9, the CARMA paralogs and its invertebrate CARD-CC homologs.

B) Functional conservation of the cnidarian CARD-CC protein in MALT1-dependent NF-κB induction

C) A representative tree (MUSCLE+PhyML) of Zap70/Syk homologs

Figure 5
Co evolution and proposed signaling model

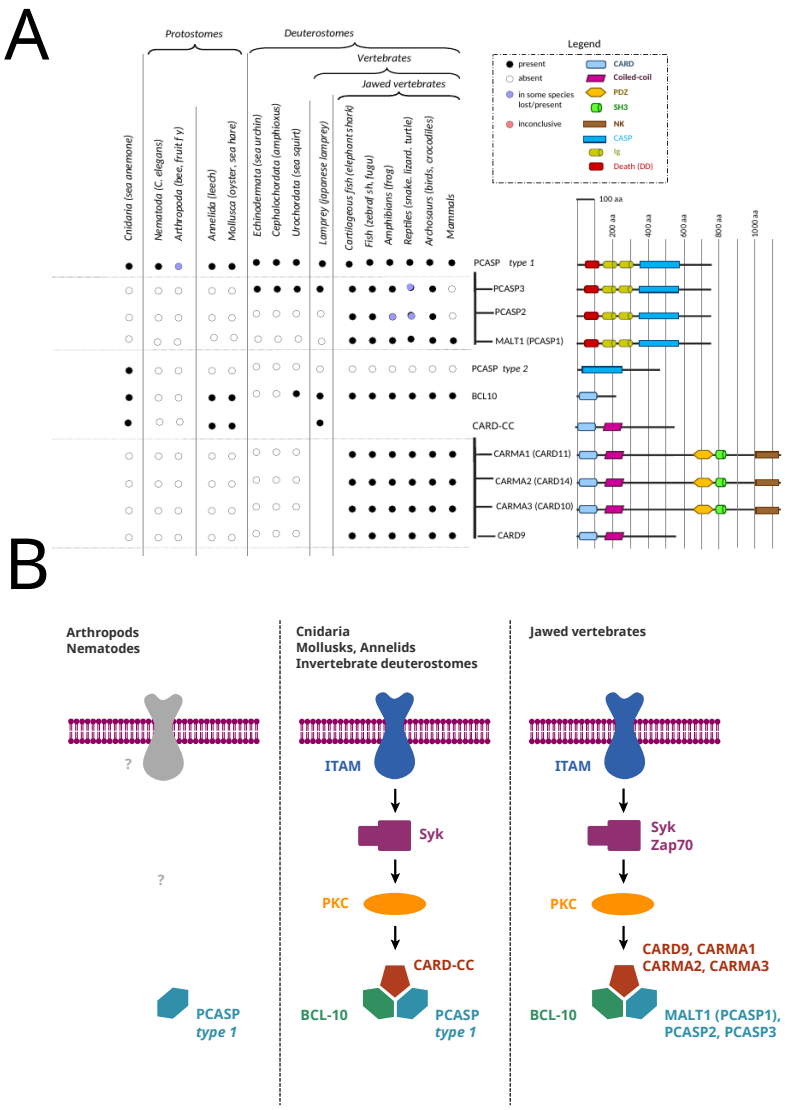

A) Patterns of co-evolution of Syk and the CBM complex components in various organisms.
B) proposed signaling model in various organism classes. Nothing is known about upstream activators of type 1 paracaspases in CARD-CC / Bcl10-independent organisms such as arthropods and nematodes.

Figure 6

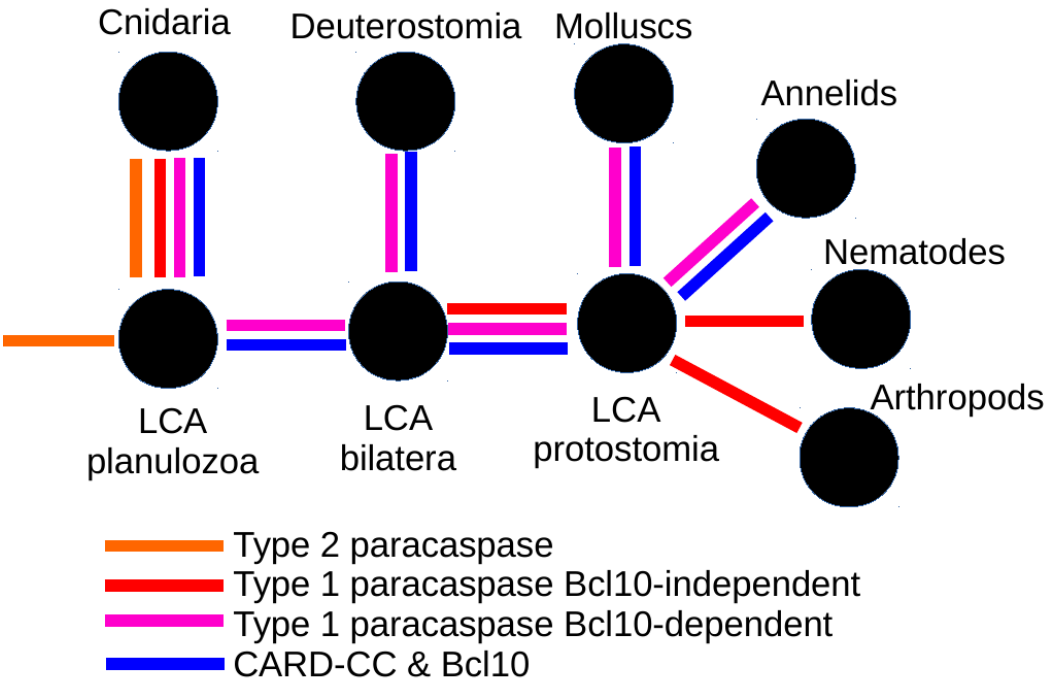

A model that proposes 2 ancient type 1 paracaspases, one Bcl10-dependent and one Bcl10-independent. The CARD-CC/Bcl10-dependent type 1 paracaspase shows MALT1-like activities. Deuterostomia (including tunicates, lancelets, vertebrates and hemichordates), annelids and mollusks inherited the Bcl10-dependent type 1 paracaspase whereas most other bilateran invertebrates kept the Bcl10-independent type 1 paracaspase. The model is based on currently available reliable sequence information and might change with additional data.